Computation of Non-Divergent Streamfunction and Irrotational Velocity Potential from the Observed Winds

J. SHUKLA[1] AND K. R. SAHA

Indian Institute of Tropical Meteorology, Poona-5, India

(Manuscript received 17 May 1973, in revised form 21 January 1974).

ABSTRACT

An iterative scheme is presented to compute streamfunction and velocity potential from the observed winds. From the computed fields of streamfunction and velocity potential, the wind field is reconstructed and the reconstructed wind field is compared with the observed wind field. Such comparisons are made for the earlier methods also. The results of intercomparison among all the methods show that the root-mean-square vector error between the observed and the reconstructed total wind is minimum in the present method.

1. Introduction

It is now largely accepted that in low latitudes the flow patterns depicted by winds are more reliable than those deduced from contour analysis (Palmer, 1952; LaSeur, 1960; Yanai and Nitta, 1967). It therefore seems desirable to explore the possibility of using wind information for various diagnostic and prognostic studies pertaining to the tropical weather systems. The present study is one such attempt. Its chief aim is to resolve the observed wind field into non-divergent streamfunction and irrotational velocity potential. The streamfunction derived from the wind field may be used as input to prognostic models and also for diagnostic computations of the geopotential field by solving the reverse balance equation.

The basic approach to the problem of computation of streamfunction ψ and velocity potential χ may be briefly stated as follows:

According to the Helmholtz theorem, the horizontal wind vector $\mathbf{V}$ can be separated into solenoidal and irrotational components as follows:

$$\mathbf{V}=\mathbf{V}_\psi+\mathbf{V}_\chi=\mathbf{k}\times\nabla\psi+\nabla\chi. \tag{1.1}$$

The vertical component of the curl of Eq. (1.1) gives

$$\mathbf{k}\cdot\nabla\times\mathbf{V}=\nabla^2\psi=\zeta \tag{1.2}$$

where ζ is the vertical component of the relative vorticity. The divergence of Eq. (1.1) gives

$$\nabla\cdot\mathbf{V}=\nabla^2\chi=D \tag{1.3}$$

where D is divergence.

Vorticity ζ and divergence D are calculated from the observed wind analysis and the following Poisson type equations are solved for obtaining ψ and χ respectively

$$\nabla^2\psi=\zeta \tag{1.4}$$

$$\nabla^2\chi=D. \tag{1.5}$$

The above equations (1.4) and (1.5) are sufficient to get ψ and χ for an infinite domain. However, the problem of finding ψ and χ for a restricted region reduces to that of specifying suitable boundary conditions. It was pointed out by Miyakoda (1960a) that the distributions of ψ and χ have no physical significance of their own and that it is only the gradients of ψ and χ constituting the wind components which have significance.

Generally, the types of boundary conditions that are used for the solution of Poisson equations (Morse and Feshback, 1953) are either Dirichlet type or Neumann type or mixed type. In meteorological problems, however, no information about ψ or χ is available at the boundaries of the computational domain and therefore various means of satisfying the following boundary conditions are considered. In

$$\mathbf{n}\cdot\mathbf{V}=V_n=-\frac{\partial\psi}{\partial s}+\frac{\partial\chi}{\partial n} \tag{1.6}$$

$$\mathbf{s}\cdot\mathbf{V}=V_s=\frac{\partial\psi}{\partial n}+\frac{\partial\chi}{\partial s}, \tag{1.7}$$

n is distance on the earth normal to the boundary increasing outward and S is distance on the earth along the boundary positive in the counter-clockwise sense. The various attempts which have been made to compute ψ and χ correspond to various degrees of approxi-

[1] Present affiliation: Geophysical Fluid Dynamics Program, Princeton University, U. S. A.

mations which are introduced to satisfy (1.6) and (1.7) at the boundary. These are reviewed in the next section. It may, however, be pointed out that the previous studies do not give any comprehensive discussion about the criteria for determining the goodness of the methods of specifying the boundary condition and computing the streamfunction. Hawkins and Rosenthal (1965) have used the criterion of root-mean-square vector error (r.m.s.v.e.) between the observed wind and the reconstructed wind. On the other hand, Sangster (1960) and Yanai and Nitta (1967) have stated that the boundary condition should be so chosen as to maximize the portion of kinetic energy (K.E.) carried by $\mathbf{V}_\psi$ and to minimize that of $\mathbf{V}_\chi$. Although this criterion seems to be arbitrary, it is simple to show that the minimum r.m.s.v.e. and maximum K.E. for the reconstructed wind field correspond to each other provided that the correlation between the observed wind and the error between the observed and the recomputed wind is negligible.

In the present study, a new method of specifying the boundary condition is suggested and ψ and χ are computed using this method. From the computed fields of ψ and χ, the wind field is reconstructed and the r.m.s.v.e. and the percentage of K.E. are computed. The results of these computations are compared with those of earlier methods and it is found that the r.m.s.v.e. between the observed and the reconstructed total wind is minimum in the present method.

2. Review of the earlier methods

Phillips (1958) made use of Eq. (1.6) in modified form to compute the boundary values of ψ. In this computation the mean value of the normal velocity V_n for all the points along the boundary was subtracted from the observed value of V_n at every point on the boundary and the boundary value of ψ was obtained by integrating the equation

$$\frac{\partial \psi}{\partial s} = -(V_n - \bar{V}_n)$$

where

$$\bar{V}_n = \oint V_n ds \Big/ \left(\oint ds\right).$$

In order to integrate the above equation along the boundary, one of the corner points is arbitrarily assigned the value of $\psi=0$ and the above equation is trapezoidally integrated to get ψ at all points of the boundary. Eq. (1.4) is then solved to get ψ for the whole region.

It may be remarked that the above method of modifying the boundary values of V_n reduces the mean divergence over the area enclosed by the boundary curve to zero. This method has been further used by Rosenthal (1963), Yanai and Nitta (1967), and Krishnamurti (1968). It was, however, shown by Hawkins and Rosenthal (1965) that this method is not satisfactory and causes large departures between the original and the reconstructed wind fields. Hereafter this method will be referred to as Method II. Solution of (1.4) with boundary value of ψ as zero, as used by Tangri (1966), will be referred to as Method I.

Brown and Neilon (1961) and Bedient and Vederman (1964) have used the method suggested by Phillips (1958) in a modified form. They do not subtract the mean value $\bar{V}_n$ from the observed value of V_n at every point on the boundary but they integrate the equation

$$\frac{\partial \psi}{\partial s} = -V_n,$$

using the observed value of V_n along the boundary. Since the integrated divergence over the whole area is not necessarily zero, the starting point value and the the end point value of ψ (two values at the same point) are found to be different. This difference is distributed uniformly among all the points of the boundary. It may be noted, therefore, that in this method the mean divergence over the area is not reduced to zero but is always having a finite value distributed uniformly along the boundary. This method will be hereafter referred to as Method III.

Sangster (1960) gave a detailed discussion of the means of specifying the boundary values of ψ and brought out the necessity of considering ψ and χ both, so as to satisfy (1.6) and (1.7) at the boundary. The method finally adopted by Sangster for obtaining the boundary value of ψ based on the above considerations may be summarized as follows:

i) Obtain χ by solving

$$\nabla^2\chi = D \quad (\chi=0 \text{ on the boundary}).$$

ii) Knowing the χ values, evaluate $\partial\chi/\partial n$ at the boundary points and integrate the following equation along the boundary

$$\frac{\partial \psi}{\partial s} = -V_n + \frac{\partial \chi}{\partial n}.$$

iii) Knowing the values at the boundary, obtain ψ field by solving $\nabla^2\psi=\zeta$.

This method will be referred to as Method IV in the present study.

Hawkins and Rosenthal (1965) have made the computations of ψ and χ using various versions of Dirichlet and Neumann boundary conditions following the suggestions by earlier workers. They have also computed the r.m.s.v.e. between the original wind and the reconstructed wind obtained by the different methods. These authors have concluded that keeping in view the machine time needed to perform the computations, the method suggested by Sangster (1960) is the most useful of the methods tested by them.

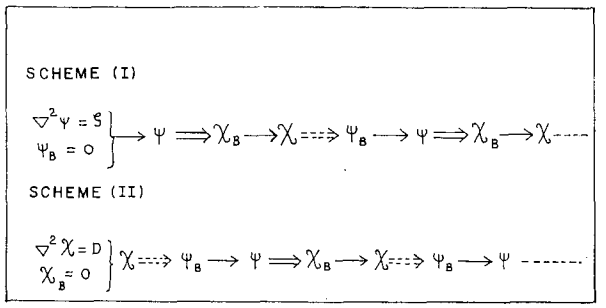

FIG. 1. Schematic representation of the iteration schemes (I) and (II). The meanings of the symbols and the arrows are as follows:

$\psi \Rightarrow \chi_B$ means, to obtain the values of χ_B from known values of ψ by integration of $\partial\psi/\partial s = V_s - \partial\psi/\partial n$ along the boundary.

$\chi \Rightarrow \psi_B$ means, to obtain the values of ψ_B from known values of χ by integration of $\partial\psi/\partial s = -V_n + \partial\chi/\partial n$ along the boundary.

$\psi_B \rightarrow \psi$ means, to obtain ψ values by relaxing $\nabla^2\psi = \zeta$ with given ψ_B.

$\chi_B \rightarrow \chi$ means, to obtain χ values by relaxing $\nabla\chi^2 = D$ with given χ_B.

3. The present method

The method suggested in the present study is essentially an extension of the Sangster method. In Sangster's method it is intended to satisfy the equation,

$$\frac{\partial\psi}{\partial s} = -V_n + \frac{\partial\chi}{\partial n}, \text{ at the boundary}$$

and

$$\nabla^2\psi = \zeta, \text{ in the interior region.}$$

Since both these equations are derived directly from Eq. (1.1), there is no approximation introduced in this procedure. Evaluation of $\partial\chi/\partial n$, however, requires knowledge of the distribution of χ, which is obtained in Sangster's method by solving the equation

$$\nabla^2\chi = D, \quad \text{with} \quad \chi = 0 \text{ at the boundary.}$$

This choice of boundary condition for χ is arbitrary and it introduces arbitrariness in the computation of χ which is further used for computation of ψ. In the present method, it is proposed to consider this limitation as the first approximation only and just as ψ is obtained at the boundary by integrating equation (1.6), similarly χ at the boundary may also be obtained by integrating equation (1.7) along the boundary using the previously obtained values of ψ to evaluate $\partial\psi/\partial n$. It may be reasonable to expect that χ values at the boundary obtained by integrating (1.7) may be more realistic than the earlier assumption of $\chi = 0$ at the boundary and therefore a more realistic χ field may be obtained by relaxing the equation (1.5) with the boundary values of χ obtained in the above-mentioned way. The new value may be used then to evaluate $\partial\chi/\partial n$ in Eq. 16 which may be integrated again to get new ψ values at the boundary. These new ψ values at the boundary may be used for solving the equation (1.4) to get a new ψ distribution. These new ψ values may be further used in the way described above to get new χ values and thus series of iterations may be performed to get values of ψ and χ. This iteration scheme, in a general form, may be schematically represented as shown in Fig. 1. Schemes I and II correspond to starting the iteration with boundary values $\psi_B = 0$ and $\chi_B = 0$ respectively, where the suffix B denotes boundary. The results of computation with Scheme I as well as a combination of Schemes I and II showed large r.m.s.v.e. between the observed and reconstructed wind fields. Scheme II gave the best results. Hence Scheme II was adopted and extended in the present study as shown schematically in Fig. 2. Here, the symbols and notations have the same meanings as in Fig. 1 but in the iterative procedure the numbers 1, 2, 3, . . ., m correspond to the different combinations of ψ and χ at different stages of iteration.

It may be seen that $m = 1$ corresponds to the method suggested by Sangster (1960). An attempt is made in the present study to extend the iteration further and compare the results at successive stages of iteration so as to find, if possible, a value of m for which the r.m.s.v.e. between the observed wind and the reconstructed total wind will be the minimum. As will be shown in subsequent sections, this criterion is met for a value of $m = 4$. Hence the present method will be described as Method IV ($m = 4$), while that of Sangster (1960) will be referred to as Method IV ($m = 1$).

4. Computations and results

a. Computational scheme

Centered space differencing is adopted for calculation of the finite-difference analogs of vorticity and divergence. The finite-difference form of the Laplacian which is used in the present study is the nine-point Laplacian suggested by Miyakoda (1960b). This form for Lapla-

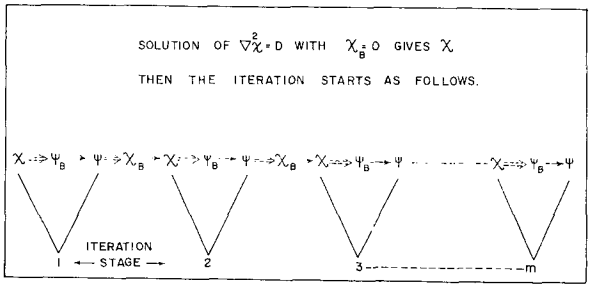

FIG. 2. Schematic representation of ψ and χ combinations at different stages of iteration. Symbols have the same meanings as those in Fig. 1.

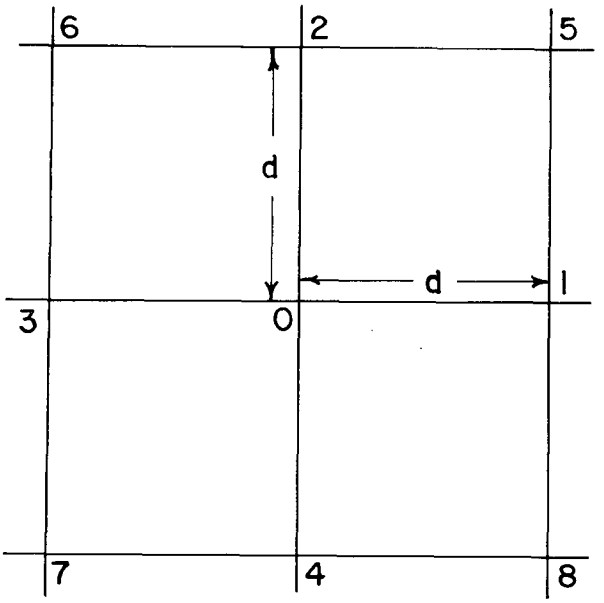

FIG. 3. Arrangement and numbering of points in a horizontal finite difference grid.

cian ψ is as follows:

$$\nabla^2\psi \equiv (2^+\nabla^2\psi + {}^\times\nabla^2\psi)/3, \tag{4.1}$$

where

$$+\nabla^2\psi = \frac{\psi_1+\psi_2+\psi_3+\psi_4-4\psi_0}{d^2}$$

$$\times\nabla^2\psi = \frac{\psi_5+\psi_6+\psi_7+\psi_8-4\psi_0}{2d^2},$$

where d is the grid-length and the suffixes refer to points shown in Fig. 3.

Eqs. (1.4) and (1.5) are solved using the above finite-difference scheme and the accelerated Liebmann relaxation technique. The most appropriate value of the over-relaxation co-efficient was determined by experiment. Fig. 4, which gives the results of this experiment, shows that the convergence is fastest for an over-relaxation coefficient of 0.7. This value is comparable with that found earlier by Miyakoda (1962).

For evaluation of ψ at the boundary by using Eq. (1.6) the χ-field is first determined by solving the Poisson equation, $\nabla^2\chi = D$, with $\chi = 0$ at the boundary. From the χ field thus obtained, $\partial\chi/\partial n$ at the boundary is evaluated by using the formula

$$\left(\frac{\partial\chi}{\partial n}\right)_0 = 2\left(\frac{\partial\chi}{\partial n}\right)_1 - \left(\frac{\partial\chi}{\partial n}\right)_2, \tag{4.2}$$

where the subscript 0 refers to the boundary and subscripts 1, 2, and 3 refer to the points which are one, two, and three grid-lengths interior to the boundary respectively, and

$$\left(\frac{\partial\chi}{\partial n}\right)_1 = (\chi_0-\chi_2)/2\Delta n$$

$$\left(\frac{\partial\chi}{\partial n}\right)_2 = (\chi_1-\chi_3)/2\Delta n,$$

where Δn is the grid-length along the n direction. It may be seen that the above-mentioned formula for $(\partial\chi/\partial n)_0$ corresponds to linear extrapolation of $\partial\chi/\partial n$ from inner to outer grid-points. It has been found by trial and error that this version of evaluation of $(\partial\chi/\partial n)_0$ gives the best results.

The boundary values V_s and V_n in Equations (1.6) and (1.7) are required to satisfy the integral constraints:

$$\int\int_A \zeta dxdy = \oint V_s ds \tag{4.3}$$

$$\int\int_A D dxdy = \oint V_n ds \tag{4.4}$$

where A denotes the area of computation. The values of V_s and V_n are suitably altered so as to satisfy the above constraints. The modification is always seen to improve the results.

b. Verification parameters

In the present paper, the following verification parameters are calculated:

i) Kinetic energy (per unit area) of the observed wind, (K_0),

$$K_0 = [\sum_{i=1}^{N} (u_0^2+v_0^2)_i]/N.$$

ii) Kinetic energy (per unit area) of the recomputed nondivergent wind, (K_ψ),

$$K_\psi = [\sum_{i=1}^{N} (u_\psi^2+v_\psi^2)_i]/N.$$

iii) Kinetic energy (per unit area) of the recomputed total wind, $(K_{\psi+\chi})$,

$$K_{\psi+\chi} = [\sum_{i=1}^{N} (u_{\psi+\chi}^2+v_{\psi+\chi}^2)_i]/N.$$

iv) Root-mean-square vector error between the observed and the recomputed non-divergent wind, (E_ψ),

$$E_\psi = [\sum_{i=1}^{N} \{(u_0-u_\psi)^2+(v_0-v_\psi)^2\}_i]/N.$$

v) Root-mean-square vector difference between the observed wind and the reconstructed total wind, $(E_{\psi+\chi})$,

$$E_{\psi+\chi}=[\sum_{i=1}^{N}\{(u_0-u_{\psi+\chi})^2+(v_0-v_{\psi+\chi})^2\}_i]/N,$$

where N is the total number of grid-points considered for the verification, and $u_{\psi+\chi}=u_\psi+u_\chi$ and $v_{\psi+\chi}=v_\psi+v_\chi$.

c. Data and area of computation

The basic data for computations consist of wind direction and speed at 2.5° latitude-longitude grid-points, picked up from manually-analyzed streamline-isotach charts. The area of computation extends from 50E to 100E and from 2.5N to 40N, as shown in Fig. 5. In the present study, data for 700 mb and 500 mb only have been used. Although the computations have been performed for several map times, the results are presented for four days only. These days are 1 and 2 July 1963, and 18 and 19 December 1968. Some results are also presented for the period 24–27 December 1968.

Computations were performed on the CDC 3600 computer available at the Tata Institute of Fundamental Research, Bombay.

d. Results

The results of computation by methods I–IV described in the present paper are presented in Tables 1–4 respectively. A significant feature of these results

TABLE 1. Results of computation by Method I.

Date	K_0 m² sec⁻²	K_ψ m² sec⁻²	$K_{\psi+\chi}$ m² sec⁻²	E_ψ m sec⁻¹	$E_{\psi+\chi}$ m sec⁻¹
1/ 7/63	38.424	16.297	20.642	4.824	4.320
2/ 7/63	45.207	16.835	21.011	5.308	4.803
18/12/68	132.442	50.79	52.209	9.101	8.018
19/12/68	132.325	58.256	58.657	7.601	7.600

TABLE 2. Results of computation by Method II.

Date	K_0 m² sec⁻²	K_ψ m² sec⁻²	$K_{\psi+\chi}$ m² sec⁻²	E_ψ m sec⁻¹	$E_{\psi+\chi}$ m sec⁻¹
1/ 7/63	38.424	40.418	39.717	4.670	3.487
2/ 7/63	45.207	42.685	43.478	4.175	3.00
18/12/68	132.445	144.765	141.573	3.820	3.134
19/12/68	132.325	160.780	154.484	3.145	2.326

TABLE 3. Results of computation by Method III.

Date	K_0 m² sec⁻²	K_ψ m² sec⁻²	$K_{\psi+\chi}$ m² sec⁻²	E_ψ m sec⁻¹	$E_{\psi+\chi}$ m sec⁻¹
1/ 7/63	38.424	41.514	40.780	4.749	3.587
2/ 7/63	45.207	40.447	41.397	3.981	2.741
18/12/68	132.442	148.518	144.514	3.266	2.253
19/12/68	132.325	161.823	155.463	3.189	2.369

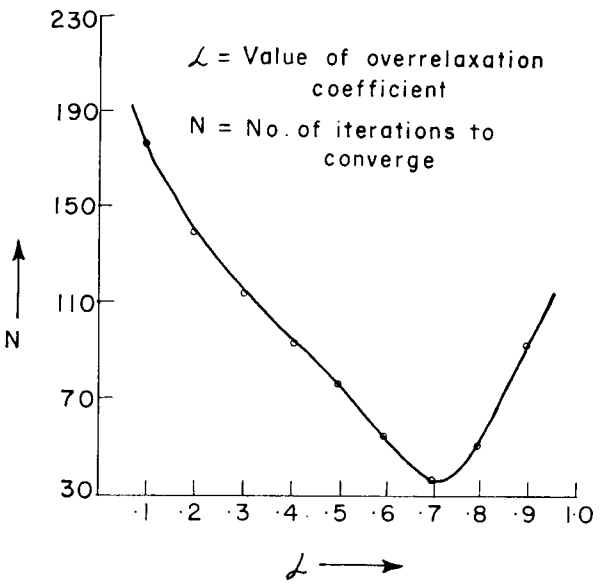

FIG. 4. Number of iterations required for convergence for different values of over-relaxation coefficient.

is that in every case $E_{\psi+\chi}$ is smaller than E_ψ and that $|K_0-K_{\psi+\chi}|$ is also always smaller than $|K_0-K_\psi|$ which means that the inclusion of the χ component always improves the results, i.e., $\mathbf{V}_{\psi+\chi}$ always gives a better representation of the original observed wind than $\mathbf{V}_\psi$ alone.

While discussing Table 4 which gives the results of computation by Method IV for $m=1$ and $m=4$, it should be pointed out that as a rule the iterations of Scheme II are continued up to $m=20$. The verification parameters are computed at every stage and stored in computer memory. The value of $E_{\psi+\chi}$ at each stage is compared with that at the previous stage and the iteration is terminated after $E_{\psi+\chi}$ has crossed the minimum. In order to see if there is more than one minimum for $E_{\psi+\chi}$ with respect to m, some calculations were extended up to $m=100$. In all the cases, however, it was found that the minimum of $E_{\psi+\chi}$ occurred at $m=4$ only. In fact, a study of the verification parameters revealed the following general features:

TABLE 4. Results of computation by Method IV.

Date	K_0 m² sec⁻²	K_ψ m² sec⁻²	$K_{\psi+\chi}$ m² sec⁻²	E_ψ m sec⁻¹	$E_{\psi+\chi}$ m sec⁻¹
1/ 7/63	$m=1$ 38.4	26.078	29.710	2.639	1.281
	$m=4$ 38.4	22.830	30.165	3.083	1.270
2/ 7/63	$m=1$ 45.2	31.213	34.782	2.791	1.438
	$m=4$ 45.2	26.537	37.950	3.120	1.361
18/12/68	$m=1$ 132.4	123.284	121.238	2.435	1.485
	$m=4$ 132.4	117.177	122.432	3.076	1.476
19/12/68	$m=1$ 132.3	132.535	127.435	2.328	1.461
	$m=4$ 132.3	141.770	130.251	3.293	1.413

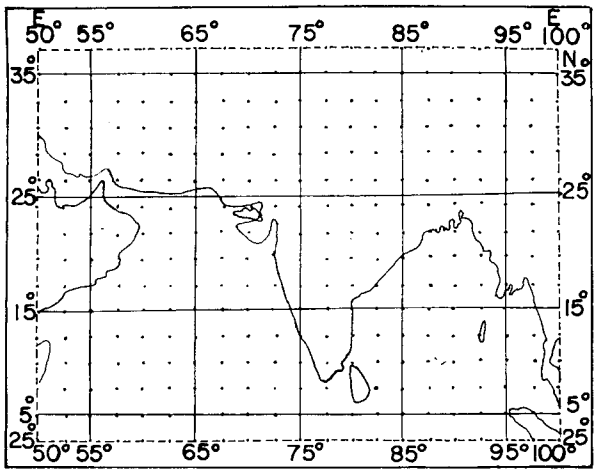

FIG. 5. Area of computation and distribution of grid-points.

i) The minimum values of E_ψ and $E_{\psi+\chi}$ did not occur at the same stage. The same was the case for the maximum values of κ_ψ and $K_{\psi+\chi}$.
ii) E_ψ was generally minimum for $m=1$ and then it started diverging for higher values of m.
iii) $E_{\psi+\chi}$ was minimum for $m=4$ and then the value started diverging out.

It may, however, be pointed out that the outcome of the present study is not to conclude that the minimum of $E_{\psi+\chi}$ will always occur at the stage $m=4$. It may occur at any other value of m also. However, in the cases studied in the present paper, the minimum value of $E_{\psi+\chi}$ occurred at $m=4$.

5. Effect of enlarging the area of computation

In order to study the effect of enlarging the area of computation, two sets of computations were performed for two different sizes of the area of computation. First set of the computations was made for a 21×16 grid (21 grid points along x-axis and 16 grid points along y-axis) as shown in Fig. 5. For this set of computations, data for the area between 50E to 100E and 2.5N to 40N were used. The root-mean-square vector error between the observed and recomputed wind was calculated for the whole area excluding the outermost two grids from all the four sides. The r.m.s.v.e. value was also calculated only for the Indian region extending from 10N to 27.5N and from 70E to 90E and this smaller area will be, hereafter, referred to as the inner verification area.

Another set of computations was performed for a larger area so that the outer boundary is removed away from the inner verification area. This set of computations was made for 41×20 grid using the data for the area between 20E and 120E and 2.5N and 50N. Error computations were compared with the error values for the inner verification area as in the first set of computations.

TABLE 5. Intercomparison between the results of smaller and bigger area of computation.

Date	Area considered	E_ψ m sec^{-1}	$E_{\psi+\chi}$ m sec^{-1}
24/12/68	Smaller area (21×16)	2.778	1.924
	Larger area (41×20)	2.622	1.623
25/12/68	Smaller area (21×16)	3.312	2.026
	Larger area (41×20)	2.872	1.771
26/12/68	Smaller area (21×16)	3.148	1.891
	Larger area (41×20)	3.064	1.813
27/12/68	Smaller area (21×16)	3.998	2.834
	Larger area (41×20)	2.983	1.831

Table 5 gives the results of computations for both the areas. These computations correspond to the stage $m=1$ in Section 4. It is seen that there is an improvement in the result after removing the boundary away from the inner verification area. These results, however, should be accepted only with caution because the effect may not be purely due to removal of the boundary away from the verification area but also due to observed values of the wind at the boundary.

6. Results of intercomparison among the methods

Table 6 gives the value E_ψ and $E_{\psi+\chi}$ for the several methods for which the computations have been made. It may be recalled that all the results mentioned in Table 6 are for the same area of computation and therefore permit an intercomparison among themselves.

TABLE 6. Intercomparison among the results for different methods of computing ψ and χ.

Date	Methods	E_ψ (m sec^{-1})	$E_{\psi+\chi}$ (m sec^{-1})
1/ 7/63	Method I	4.824	4.320
	Method II	4.670	3.487
	Method III	4.749	3.587
	Method IV $m=1$	2.639	1.281
	Method IV $m=4$	3.083	1.270
2/ 7/63	Method I	5.308	4.803
	Method II	4.175	3.000
	Method III	3.981	2.741
	Method IV $m=1$	2.791	1.438
	Method IV $m=4$	3.120	1.361
18/12/68	Method I	8.101	8.018
	Method II	3.820	3.134
	Method III	3.266	2.253
	Method IV $m=1$	2.435	1.485
	Method IV $m=4$	3.076	1.476
19/12/68	Method I	7.601	7.600
	Method II	3.145	2.326
	Method III	3.189	2.369
	Method IV $m=1$	2.328	1.461
	Method IV $m=4$	3.293	1.413

Compared to other methods, Method I gives the highest values of E_ψ as well as $E_{\psi+\chi}$ for all the days. Method IV gives the lowest values of E_ψ and $E_{\psi+\chi}$ for all the days. Methods II and III give results which are better than Method I but worse than Method IV. Between Methods II and III, the result depends upon the synoptic situation which implies the distribution of V, ζ and D. In method IV, the values of E_ψ for $m=1$ is always less than the value of E_ψ for $m=4$ but the value of $E_{\psi+\chi}$ for $m=4$ is always less than the value of $E_{\psi+\chi}$ for $m=1$ .This result was also found for the computations of several other map times which have not been reported here. This result leads us to the conclusion that the error between the observed and the reconstructed nondivergent wind is always minimum for $m=1$ and the error between the observed and the reconstructed total wind is always minimum for $m=4$. It may be further noted that various other combinations of ψ and χ were also tried but the results did not improve. In particular, the total reconstructed wind was obtained by combining ψ for $m=1$ and χ for $m=4$ but the results were found to be worse than the case in which ψ and χ both were taken for $m=4$. Similarly ψ for $m=1$ was combined with χ for $m=1, 2, 3, 4, \ldots$, etc., but the results did not improve over the results presented in the preceding section for $m=1$ and $m=4$.

7. Conclusions

From the study of the results of computations by all the methods using data of several map times and from their intercomparisons the following conclusions may be drawn:

i) For the computation of ψ and χ there appears to be no unique method of specifying the boundary conditions.

ii) The results of computations of ψ and χ appear to depend upon:
   a) Type of boundary condition
   b) Type of finite difference scheme used to evaluate the differentials
   c) Type of synoptic situation which implies the type of distribution of wind, vorticity, and divergence fields
   d) Relative magnitudes and distribution of vorticity and divergence.

iii) There is some improvement in the results by removing the boundary of computation away from the area of verification.

iv) There is no unique way of making intercomparison among the various methods of computing ψ and χ. However, the criterion of minimum root-mean-square vector error between the observed and the reconstructed wind is found to be suitable for the purpose.

v) The computations with $\psi=0$ as the boundary condition give the worst results.

vi) The root-mean-square vector error between the observed and reconstructed nondivergent wind is minimum for $m=1$ of Method IV.

vii) The method suggested in the present study ($m=4$ of Method IV) gives minimum root-mean-square error between the observed and the reconstructed total wind.

Acknowledgment. The authors' grateful thanks are due to Mrs. A. A. Kulkarni and Mr. P. S. Nayar for their general assistance in the preparation of this paper, to Mr. R. S. Sonawane for efficient typing of the manuscript, and to Mr. S. D. Parnaik and Mr. A. S. Gade for preparing the diagrams.

REFERENCES

Bedient, H. A., and J. Vederman, 1964: Computer analysis and forecasting in the tropics. *Mon. Wea. Rev.*, **92**, 565–577.

Brown, J. A., and J. R. Neilon, 1961: Case studies of numerical wind analysis. *Mon. Wea. Rev.*, **89**, 83–90.

Hawkins, H. F., and S. L. Rosenthal, 1965: On the computation of stream functions from the wind field, *Mon. Wea. Rev.*, **93**, 245–252.

Krishnamurti, T. N., 1968: A diagnostic balance model for studies of weather systems of low and high latitudes, Rossby number less than 1. *Mon. Wea. Rev.*, **96**, 197–207.

LaSeur, N. E., 1960: Methods of tropical synoptic analysis. *Proc. Symposium on Tropical Meteorology*, Nairobi, 1960, pp. 24–34.

Miyakoda, K., 1960a: Numerical solution of the balance equation. Japan Meteor. Agency, Tech. Report No. 3, pp. 15–34.

——, 1960b: Numerical calculation of Laplacian and Jacobian using 9 and 25 grid point system. Collected Meteorological Papers, Japan, Vol. **10**, No. 1–2, 125 pp.

——, 1962: Contribution to the numerical weather prediction, Computation with finite difference. *Japanese Jour. Geophys.*, **3**, 75–190.

Morse, P. M., and H. Feshback, 1953: *Methods of Theoretical Physics*. New York, McGraw-Hill Book Co., Inc.

Palmer, C. E., 1952: Tropical meteorology. *Quart. J. Roy. Meteor. Soc.*, **78**, 126–164.

Phillips, N. A., 1958: Geostrophic errors in predicting the Appalachian storm of Nov. 1950. *Geophysica*, **5**, 389–405.

Rosenthal, S. L., 1963: A barotropic model for prediction in the tropics, United States Asian Military Weather Symposium, John Hay Air Base, Phillipine Islands.

Sangster, W. E., 1960: A method of representing the horizontal pressure force without reduction of pressures to sea level. *J. Meteor.*, **17**, 166–176.

Tangri, A. C., 1966: Computation of streamlines associated with a low latitude cyclone. *Indian J. Meteor. Geophys.*, **17**, 401–406.

Yanai, M., and T. Nitta, 1967: Computation of vertical motion and vorticity budget in a Caribbean easterly wave. *J. Meteor. Soc. Japan*, **45**, December 444–466.